Computational and Structural Biotechnology Journal 19 (2021) 2318–2328

COMPUTATIONAL AND STRUCTURAL BIOTECHNOLOGY JOURNAL

journal homepage: www.elsevier.com/locate/csbj

Identification of the key target profiles underlying the drugs of narrow therapeutic index for treating cancer and cardiovascular disease

Jiayi Yin [a,1], Xiaoxu Li [a,1], Fengcheng Li [a], Yinjing Lu [a], Su Zeng [a,b,*], Feng Zhu [a,b,c,*]

[a] College of Pharmaceutical Sciences, Zhejiang University, Hangzhou 310058, China
[b] Innovation Institute for Artificial Intelligence in Medicine of Zhejiang University, Hangzhou 310018, China
[c] Alibaba-Zhejiang University Joint Research Center of Future Digital Healthcare, Hangzhou 330110, China

ARTICLE INFO

Article history:
Received 16 December 2020
Received in revised form 9 April 2021
Accepted 15 April 2021
Available online 21 April 2021

Keywords:
Narrow therapeutic index
Cancer
Cardiovascular disease
Artificial intelligence
Drug mechanism

ABSTRACT

An appropriate therapeutic index is crucial for drug discovery and development since narrow therapeutic index (NTI) drugs with slight dosage variation may induce severe adverse drug reactions or potential treatment failure. To date, the shared characteristics underlying the targets of NTI drugs have been explored by several studies, which have been applied to identify potential drug targets. However, the association between the drug therapeutic index and the related disease has not been dissected, which is important for revealing the NTI drug mechanism and optimizing drug design. Therefore, in this study, two classes of disease (cancers and cardiovascular disorders) with the largest number of NTI drugs were selected, and the target property of the corresponding NTI drugs was analyzed. By calculating the biological system profiles and human protein–protein interaction (PPI) network properties of drug targets and adopting an AI-based algorithm, differentiated features between two diseases were discovered to reveal the distinct underlying mechanisms of NTI drugs in different diseases. Consequently, ten shared features and four unique features were identified for both diseases to distinguish NTI from NNTI drug targets. These computational discoveries, as well as the newly found features, suggest that in the clinical study of avoiding narrow therapeutic index in those diseases, the ability of target to be a hub and the efficiency of target signaling in the human PPI network should be considered, and it could thus provide novel guidance in the drug discovery and clinical research process and help to estimate the drug safety of cancer and cardiovascular disease.

1. Introduction

A narrow therapeutic index (NTI) of a drug implies that a tiny variation in the dosage of the drug might lead to treatment failure or severe adverse drug reactions [1–5]. It also hampers drug development since researchers have to conduct additional studies [6] to modify the compound structure, and some failures in drug research [7] are caused by the NTI of drug candidates. In the course of clinical research, some NTI drugs pose great risks in clinical use due to the lack of clear dose adjustment recommendations [4,8]. It is essential to start mitigation methods to avoid unfavorable traits or to potentially alter resources to alternative candidates by gaining an early consideration of the likely TI value of a certain drug [9–10]. Moreover, this is critical for avoiding clinical trials because TI with low indication specificity may be considered morally unacceptable [2]. Therefore, the molecular mechanisms of NTI drugs play a prominent role in pharmaceutical discovery and clinical research and help to estimate drug safety and efficacy [11].

However, it is complicated to determine and interpret the TI of a drug because this depends not only on the stage of development that affects the available data but also on the properties of the indications for which the drug is being developed [2,12]. A widely used concept of TI is the quantitative relationship between pharmacology and safety toxicology, but the definition of a therapeutic or toxic effect is highly dependent on different therapeutic and toxic effect types [3]. For example, imatinib can allow more toxicity with a smaller TI value when used in cancer in pursuit of higher pharmacological exposure, but there must be a larger and more reasonable TI value when used for pulmonary hypertension [2,13]. This adds complexity to the understanding of the molecular mechanisms of NTI drugs. In fact, of the 161 NTI drugs currently FDA approved, almost half of them belong to cancer and cardiovascular

* Corresponding authors at: College of Pharmaceutical Sciences, Zhejiang University, Hangzhou 310058, China.
[1] These authors contributed equally to this work as first authors.

https://doi.org/10.1016/j.csbj.2021.04.035

disease. Cancer is a group of diseases characterized by uncontrolled cell growth. The cardiovascular disease usually involves narrowed or blocked blood vessels, which can contribute to heart attack, angina, or stroke and is characterized by acute onset, critical condition, and rapid progression [14]. These observations suggest that there may be disease-specific pathology, resulting in different types of the disease each with its characteristics [15], and the molecular mechanisms of NTI drugs in different diseases may also exhibit large variations. Therefore, when designing drugs and conducting clinical research on these two types of diseases, it is necessary to consider the different molecular mechanisms of NTI drugs between them.

To enhance the understanding of TI, a variety of studies and some approaches have been developed to enhance the ability to reveal the mechanism underlying NTI drugs, such as the exposure-centric TI approach [2], preclinical pharmacology model [16–18], assessment of off-target safety margins [19]. Recently, an article was published in *Frontiers in Pharmacology* [20] using a target-based approach, combining the profiles of human protein–protein interaction (PPI) network, and biological systems to find features or feature groups that can be used to indicate the drug's narrow TI. It identified 8 features that could collectively indicate that NTI drug targets are tremendously connected and centralized and are related to target druggability in all diseases. Agnieszka Potęga, et al. [21] have shown that this target-based approach to study the mechanisms underlying NTI drugs is important to indicate a well-balanced profile between efficacy and safety. However, no studies have revealed the underlying mechanism behind the complex definition and interpretation of TI in different diseases, and what significantly limits NTI drug design and clinical studies for both specific diseases, and this needs to be solved urgently.

Therefore, in this study, the underlying mechanisms of NTI drugs aimed at cancer and cardiovascular disease were analyzed based on not only the human PPI network features but also the biological system profiles. To discover this underlying mechanism, the NTI and NNTI drug targets were divided into three groups: (i) NTI drug targets of cancer, (ii) NTI drug targets of cardiovascular disease, and (iii) NNTI drug targets for all indications. Next, through the comparative analysis of the target groups (i) and (iii) and the target groups (ii) and (iii), several essential features that could distinguish the two groups were identified, and further studies revealed similarities and differences in the characteristics of cancer and cardiovascular disease. Overall, these findings combined with the newly recognized features can indicate the underlying mechanisms of NTI drugs targeting cancer and cardiovascular disease, respectively, which offer certain guidance in assessing the risks and benefits of drug candidates, as well as drug discovery and clinical research in cancer and cardiovascular disease.

2. Materials and methods

2.1. NTI drugs collection and associated targets and indications identification

The NTI approved drugs and their related drug targets and indications were obtained through the following steps. First, 1,921 FDA approved drugs with their related indications were systematically collected and identified from the orange book of the US FDA [72]. Then, all the corresponding diseases were standardized by the ICD-11 codes (the latest version of the International Classification of Diseases) [73]. Next, the corresponding targets of the approved drugs were authorized by the therapeutic target database (TTD) [74], and 506 corresponding targets of the approved drugs were confirmed. Third, a systematic literature review of all these drugs was performed to confirm their TI value by searching the PubMed database using such keyword combinations as "Drug Name/Synonym" + "Therapeutic ranges" / "Therapeutic index" / "Therapeutic ration" / "Therapeutic window". Consequently, 36 NTI drugs targeting cancer and 18 NTI drugs targeting cardiovascular disease are discovered, which account for approximately half of all NTI drugs. Moreover, 29 NNTI drugs targeting all indications are also distinguished. The FDA-approved NTI drugs for cancer and cardiovascular disease together with their standardized indication, ICD-11 codes, and targets are provided in Table 1, and the NNTI drugs for all indication together with their standardized indication, ICD-11 codes, and targets are provided in Table 2.

2.2. Assessing the profile of human PPI network properties and biological systems for corresponding therapeutic targets

The human PPI network properties studied in this research consisted of 15,554 proteins and 642,304 interactions between these proteins, and these were created via the information furnished by the STRING database [75]. Only those protein interactions with confidence above 0.95 were selected for further analysis to guarantee the dependability of the analytical data [76–77]. Thus, in this study, a subnetwork consisting of 8,509 proteins, and 40,468 interactions between these proteins was developed for subsequent study. Additionally, the PPI network characteristics of corresponding therapeutic targets were obtained by the PROFEAT [78] and the tool Network Analyzer of Cytoscape [79–80]. In summary, 32 PPI network properties were calculated for further analysis, as shown in Table 3 (six features that are all zeroes were deleted, which are: 'closeness centrality sum', 'bridging centrality', 'eigenvector centrality', 'page rank centrality', 'number of selfloops', and 'current flow closeness'). Then, the additional four features of each corresponding target in the biological system profile were estimated.

The first feature is the number of target-affiliated pathways that were collected from the KEGG database [81]. This feature was confirmed by two aspects. On the one hand, the pathway of the corresponding drug targets should be necessary for life not only for patients but also in healthy individuals. On the other hand, the therapeutic target should be upstream and have the ability to regulate the biological function of the pathway. The second feature is the number of each therapeutic drug target distributed in human tissues, which was offered in the TissueDistributionDBs [82] and UniProt [83] databases. The determination of this feature depends on a higher level of total protein (>5%) distributed in a particular tissue or a higher target concentration in that tissue than the average protein concentration. To explore the off-target collateral effect, the third feature was adopted, which is the number of human similarity proteins. This was determined by counting the number of similar proteins that are outside the target protein family for the studied drug target [84–85]. This was calculated using BLAST similarity screening with the cutoff value of e-value < 0.005 [86–87] for the human proteome method furnished in the UniProt database [83]. The differential expression of the target is the fourth feature, which is capable of reflecting the expression differences of the corresponding target between diseased and healthy populations for specific diseases [74,88–89]. The expression data were gathered from TTD [90] and calculated by using the HG-U133 Plus 2.0 platform which was determined by the Gene Expression Omnibus database [91].

Collectively, these 36 features are valuable and meaningful in revealing human protein–protein interaction data for a given target, including their connectivity, organization, robustness, and stability in the human PPI network [92–94] and the on-target and off-target pharmacology of the studied targets [85,95]. These two aspects are key to enhancing potency for characterizing the underlying mechanisms of NTI drugs [2,96]. In previous publications, including our previous analysis [20],

Table 1
FDA approved NTI drugs of cancer and cardiovascular disease together with their standardized indication, ICD-11 code, and target. **ADRA1**: Adrenergic receptor alpha 1; **ADRA2**: Adrenergic receptor alpha 2; **ADRB1**: Adrenergic receptor beta-1; **ADRB2**: Adrenergic receptor beta-2; **ADRB3**: Adrenergic receptor beta-3; **ATIII**: Antithrombin-III; **BCL-2**: Apoptosis regulator BCL-2; **F2**: coagulation factor II; **F10**: Activated coagulation factor X; **DHFR**: Dihydrofolate reductase; **TOP1**: DNA topoisomerase I; **TOP2**: DNA topoisomerase II; **EGFR**: Epidermal growth factor receptor; **ESR**: Estrogen receptor; **hDNA**: Human deoxyribonucleic acid; **IMPDH1**: Inosine-5′-monophosphate dehydrogenase 1; **IFNA2**: Interferon-alpha 2; **NET**: Norepinephrine transporter; **PDGFRB**: Platelet-derived growth factor receptor; **RET**: Proto-oncogene c-Ret; **RRM2**: Ribonucleoside-diphosphate reductase M2; **mTOR**: Serine/threonine-protein kinase mTOR; **SPT ATPase**: Sodium/potassium-transporting ATPase; **TMP1**: Thymidylate synthase; **TUB**: Tubulin; **c-Kit**: Tyrosine-protein kinase Kit; **KDR**: Vascular endothelial growth factor receptor 2; **VKORC1**: Vitamin K epoxide reductase complex 1; **SCN5A**: Voltage-gated sodium channel alpha Nav1.5; **SCN5A**: Voltage-gated sodium channel alpha Nav1.5; **SCN11A**: Voltage-gated sodium channel alpha Nav1.9.

FDA Approved Drug (Reference for NTI)	Time of Approval	FDA Approved Indication	ICD-11 Code	Disease Class	Target Name
Argatroban [22]	2000	Intracardiac thrombosis	BC46	Cardiovascular	F2
Axitinib [23]	2012	Rectum cancer	2B92	Cancer	KDR
Busulfan [24]	1954	Chronic myeloid leukemia	2B33	Cancer	hDNA
Capecitabine [25]	1998	Breast cancer	2C60	Cancer	TMP1
Carboplatin [26]	1989	Ovary cancer	2C73	Cancer	hDNA
Cisplatin [27]	1978	Ovary cancer	2C73	Cancer	hDNA
Clonidine [28]	1974	Hypertension	BA00	Cardiovascular	ADRA2
Cyclophosphamide [29]	1959	Acute myeloid leukemia	2A60	Cancer	hDNA
Dalteparin Sodium [22]	1994	Deep vein thrombosis	BD71	Cardiovascular	ATIII
Digitoxin [30]	1982	Heart failure	BD10	Cardiovascular	SPT ATPase
Digoxin [31]	1954	Heart failure	BD10	Cardiovascular	SPT ATPase
Disopyramide Phosphate [32]	1977	Ventricular tachyarrhythmia	BC71	Cardiovascular	SCN5A
Docetaxel [33]	1996	Breast cancer	2C60	Cancer	TUB
Doxorubicin HCl [34]	1974	Breast cancer	2C60	Cancer	TOP2
Epinephrine [35]	1951	Coronary artery disease	BA80	Cardiovascular	ADRB1
Epirubicin HCl [36]	1999	Axillary node cancer	2D60	Cancer	TOP2
Etoposide [37]	1983	Testis cancer	2C80	Cancer	TOP2
Etoposide Phosphate [26]	1996	Ovary cancer	2C73	Cancer	TOP2
Everolimus [38]	2009	Renal cell carcinoma	2C90	Cancer	mTOR
Flecainide Acetate [39]	1985	Arrhythmic	BC64	Cardiovascular	SCN5A
Fluorouracil [40]	1962	Colorectal cancer	2B91	Cancer	TMP1
Fondaparinux Sodium [41]	2001	Deep vein thrombosis	BD71	Cardiovascular	F10
Gefitinib [42]	2003	Lung cancer	2C25	Cancer	EGFR
Gemcitabine HCl [43]	1996	Pancreatic cancer	2C10	Cancer	RRM2
Guanethidine Monosulfate [22]	1960	Hypertensive crisis	BA03	Cardiovascular	NET
Interferon Alfa-2B [44]	1986	Melanoma	2C30	Cancer	IFNA2
Irinotecan HCl [34]	1996	Colorectal cancer	2B91	Cancer	TOP1
Lidocaine [45]	1948	Ventricular tachyarrhythmia	BC71	Cardiovascular	SCN11A
Mercaptopurine [46]	1953	Acute lymphocytic leukemia	2A82	Cancer	IMPDH1
Methotrexate Sodium [26]	1953	Breast cancer	2C60	Cancer	DHFR
Mitomycin [47]	1981	Stomach cancer	2B72	Cancer	hDNA
Mitotane [48]	1970	Adrenal gland cancer	2D11	Cancer	ESR
Oxaliplatin [49]	2002	Colorectal cancer	2B91	Cancer	hDNA
Paclitaxel [50]	1992	Kaposi sarcoma	2B57	Cancer	TUB; BCL-2
Pazopanib HCl [23]	2009	Renal cell carcinoma	2C90	Cancer	c-Kit; KDR; PDGFRB
Pemetrexed [51]	2004	Pleura cancer	2C26	Cancer	DHFR; TMP1
Pemetrexed Disodium [51]	2004	Pleura cancer	2C26	Cancer	DHFR; TMP1
Phenprocoumon [52]	1957	Intracardiac thrombosis	BC46	Cardiovascular	VKORC1
Prazosin HCl [22]	1976	Hypertension	BA00	Cardiovascular	ADRA1
Procainamide HCl [53]	1950	Ventricular tachyarrhythmia	BC71	Cardiovascular	BTX-activated cardiac channel
Propafenone HCl [22]	1989	Atrial fibrillation	BC81	Cardiovascular	ADRB1; ADRB2; ADRB3
Quinidine [22]	1950	Ventricular tachyarrhythmia	BC71	Cardiovascular	SCN5A
Regorafenib [23]	2012	Gastrointestinal stromal cancer	2B5B	Cancer	c-Kit; KDR; RET
Sorafenib Tosylate [23]	2005	Adrenal gland cancer	2D11	Cancer	EGFR; c-Kit; KDR; PDGFRB
Sotalol HCl [22]	1992	Ventricular tachyarrhythmia	BC71	Cardiovascular	ADRB1
Sunitinib Malate [23]	2006	Gastrointestinal stromal cancer	2B5B	Cancer	KDR
Teniposide [26]	1992	Acute lymphocytic leukemia	2A82	Cancer	TOP2
Thioguanine [46]	1966	Acute myeloid leukemia	2A60	Cancer	hDNA
Topotecan HCl [26]	1996	Ovary cancer	2C73	Cancer	TOP1
Vandetanib [23]	2011	Thyroid gland cancer	2D10	Cancer	EGFR; KDR; RET
Vinblastine Sulfate [39]	1965	Hodgkin lymphoma	2B30	Cancer	TUB
Vincristine Sulfate [54]	1963	Acute lymphocytic leukemia	2A82	Cancer	TUB
Vinorelbine Tartrate [55]	1994	Lung cancer	2C25	Cancer	TUB
Warfarin Sodium [31]	1954	Pulmonary thromboembolism	BB00	Cardiovascular	VKORC1

a series of analyses have been performed by these 36 features. And these 36 features (30 features are described in Table 3, excluding the 6 features that the calculated values are zero) are still adopted in this study to further explore the different features of NTI drug targets between two representative disease classes (cancers and cardiovascular diseases). Their calculation formulas and biological descriptions are separately reflected in Supplementary Table S1.

2.3. NTI drug characteristic identification in two diseases by an artificial intelligence-based algorithm

Artificial intelligence (AI) has seen significant advancement in recent decades for aiding drug treatment [97–101], predicting drug-target or drug-drug interactions [5,102–103], and optimizing treatment protocols [104–106], including machine learning algorithms [107–109], deep learning methods [110–112], and

Table 2
FDA approved NNTI drugs of all indications together with their standardized indication, ICD-11 code, and target. **ABAT**: GABA transaminase; **ACE**: Angiotensin-converting enzyme; **CACNA1G**: Voltage-gated calcium channel alpha Cav3.1; **CACNA2D1**: Voltage-gated calcium channel alpha-2/delta-1; **CACNA2D2**: Voltage-gated calcium channel alpha-2/delta-2; **CACNA2D3**: Voltage-gated calcium channel alpha-2/delta-3; **CYSLTR1**: Leukotriene CysLT1 receptor; **D2R**: Dopamine D2 receptor; **DPP4**: Dipeptidyl peptidase 4; **DPYSL2**: Dihydropyrimidinase related protein 2; **F10**: Activated coagulation factor X; **GABRA1**: GABA(A) receptor alpha-1; **GABRG3**: GABA(A) receptor gamma-3; **GAR**: Gamma-aminobutyric acid receptor; **GRIA**: Glutamate receptor AMPA; **GRIK1**: Glutamate receptor ionotropic kainate 1; **hDNA**: Human deoxyribonucleic acid; **HIV RT**: Human immunodeficiency virus Reverse transcriptase; **KCNQ2**: Voltage-gated potassium channel Kv7.2; **KCNQ3**: Voltage-gated potassium channel Kv7.3; **NET**: Norepinephrine transporter; **NMDAR**: N-methyl-D-aspartate receptor; **PPP3CA**: Calcineurin; **SCN11A**: Voltage-gated sodium channel alpha Nav1.9.; **SCN1A**: Sodium channel protein type 1 subunit alpha; **SV2A**: Synaptic vesicle glycoprotein 2A; **TACR1**: Substance-P receptor; **TOP2**: DNA topoisomerase II.

FDA Approved Drug (Reference for NTI)	Time of Approval	FDA Approved Indication	ICD-11 Code	Disease Class	Target Name
Apixaban [56]	2012	Deep vein thrombosis	BD71	Cardiovascular	F10
Aripiprazole [57]	2002	Schizophrenia	6A20	Mental disorder	D2R
Atomoxetine HCl [58]	2002	ADHD	6A05	Mental disorder	NET
Clobazam [59]	2011	Epilepsy or seizures	8A60	Nervous system	GABRA1; GABRG3
Clonazepam [22]	1975	Epilepsy or seizures	8A60	Nervous system	GABRA1
Enalapril Maleate [60]	1985	Hypertension	BA00	Cardiovascular	ACE
Ethosuximide [22]	1960	Epilepsy or seizures	8A60	Nervous system	CACNA1G
Ezogabine [59]	2011	Epilepsy or seizures	8A60	Nervous system	KCNQ2; KCNQ3
Felbamate [22]	1993	Epilepsy or seizures	8A60	Nervous system	NMDAR
Gabapentin [61]	1993	Epilepsy or seizures	8A60	Nervous system	CACNA2D2; CACNA2D3
Gabapentin Enacarbil [61]	1993	Epilepsy or seizures	8A60	Nervous system	CACNA2D2; CACNA2D3
Lacosamide [62]	2008	Epilepsy or seizures	8A60	Nervous system	DPYSL2
Lamivudine [63]	1995	HIV infection	1C62	Infection	HIV RT
Lamotrigine [22]	1994	Bipolar disorders	6A60	Mental disorder	SCN11A
Levetiracetam [22]	1999	Epilepsy or seizures	8A60	Nervous system	SV2A
Linagliptin [64]	2011	Type 2 diabetes mellitus	5A11	Metabolic disease	DPP4
Mechlorethamine HCl [65]	1949	Mature T-cell lymphoma	2A90	Cancer	hDNA
Mitoxantrone HCl [66]	1987	Multiple sclerosis	8A40	Nervous system	TOP2
Montelukast Sodium [67]	1998	Asthma	CA23	Respiratory system	CYSLTR1
Oxcarbazepine [22]	2000	Epilepsy or seizures	8A60	Nervous system	SCN11A
Perampanel [56]	2012	Epilepsy or seizures	8A60	Nervous system	GRIA
Pimecrolimus [68]	2001	Atopic eczema	EA80	Skin disease	PPP3CA
Pregabalin [69]	2004	Epilepsy or seizures	8A60	Nervous system	CACNA2D1
Rivaroxaban [59]	2011	Deep vein thrombosis	BD71	Cardiovascular	F10
Rolapitant HCl [70]	2015	Nausea or vomiting	DD90	Digestive system	TACR1
Rufinamide [62]	2008	Epilepsy or seizures	8A60	Nervous system	N.A.
Topiramate [22]	1996	Epilepsy or seizures	8A60	Nervous system	GABRA1
Vigabatrin [71]	2009	Types of seizures	8A68	Nervous system	ABAT
Zonisamide [22]	2000	Epilepsy or seizures	8A60	Nervous system	SCN1A

cognitive-computing [113]. In this study, to better understand the underlying mechanisms of NTI drugs, one of the most widely used artificial intelligence algorithms, Boruta, which was based on a random forest classifier [18,114], was adopted. This method compares the correlation between real features and random probes to determine the extension of the correlation [115]. The Boruta algorithm was built by an AI-based method (machine learning), which is particularly suitable for low-dimensional data sets in other available strategies because of its strong stability in variable selection [116–117]. Then, the different characteristics between NTI and NNTI drug targets of cancer and cardiovascular disease were determined by the R package Boruta, respectively [118]. Notably, assessing the profile of human PPI network properties and the biological system for each target was conducted using the Boruta algorithm in the R environment and setting the parameters as follows: holdHistory and mcAdj = TRUE, getImp = getImpRfZ, maxRuns = 100, doTrace = 2, p-value < 0.05. Eventually, the features that could elucidate the essential factors indicating narrow TI of drugs in cancer and cardiovascular disease were respectively selected.

3. Results and discussion

3.1. Merging the human PPI network and biological system properties for artificial intelligence-based algorithm

The drug risk-to-benefit ratio (RBR) is mainly determined by the drug target profile of the network properties and biological system [84,119–121]. Network characteristics are inherent to drug targets in human PPI networks, and biological system properties can mirror the pharmacology of on-target and off-target. In this paper, the most comprehensive sets of characteristics belong to the human PPI network properties and biological system profiles were chosen to further explore the different features of NTI drug targets between two representative diseases (cancer and cardiovascular disease). Their calculation formulas and biological descriptions are separately reflected in Supplementary Table S1. The average and median values of 30 features for cancer NTI drug targets, cardiovascular disease NTI drug targets, and NNTI drug targets were also calculated (removing six characteristics equal to 0), as shown in Table 3. These 30 features were classified into three categories according to the attributes inherent in each feature, that is, the connectivity/adjacency-based properties, the shortest path length-based properties, and the human biological system properties, as also shown in Table 3.

The mean and median values between the two groups of targets (NTI and NNTI drug targets) for each disease in Table 3 show a significant difference between the two groups of targets in many features. However, none of them can be used separately as an indicator to distinguish between NTI drug targets and NNTI drug targets. Only through collective combination can NTI drug targets be more effectively distinguished from NNTI drug targets [20]. Therefore, in the next part of the study, we integrated the feature selection method based on artificial intelligence to select some important indexes from these features that can be combined to determine the drug targets of NTI and the drug targets of NNTI. However, this approach seems to introduce a very strong bias when 36 features are directly used for feature selection because of the significant dependence between 19 of these features [20].

Table 3
The calculated mean and median values of 30 properties in the human PPI network and biological system profiles.

	Feature	Cancer				Cardiovascular Disease			
		Mean Value of Targets of the NTI	Median Value of Targets of the NTI	Mean Value of Targets of the NNTI	Median Value of Targets of the NNTI	Mean Value of Targets of the NTI	Median Value of Targets of the NTI	Mean Value of Targets of the NNTI	Median Value of Targets of the NNTI
Connectivity/ adjacency-based	Bridging coefficient	1.02E−01	4.10E−02	6.79E−01	6.10E−02	7.64E−01	1.40E−01	3.70E+00	3.23E−01
	Clustering coefficient	1.32E−01	9.90E−02	1.84E−01	7.60E−02	2.85E−01	3.17E−01	2.72E−01	1.00E−01
	Degree	2.12E+01	1.50E+01	2.07E+01	1.30E+01	5.66E+00	5.50E+00	4.92E+00	3.00E+00
	Degree centrality	2.74E−03	2.00E−03	2.64E−03	2.00E−03	7.50E−04	1.00E−03	5.49E−04	0.00E+00
	Interconnectivity	2.64E−01	2.55E−01	4.13E−01	2.69E−01	4.83E−01	4.38E−01	5.28E−01	5.00E−01
	Neighborhood connectivity	3.49E+01	2.77E+01	2.59E+01	2.04E+01	1.75E+01	1.47E+01	1.81E+01	1.13E+01
	Number of triangles	3.00E+01	1.70E+01	4.60E+01	1.50E+01	2.53E+00	2.00E+00	2.50E+00	1.00E+00
	Scaled degree	2.83E−02	2.00E−02	2.75E−02	1.70E−02	7.50E−03	7.50E−03	6.56E−03	4.00E−03
	Topological coefficient	9.63E−02	1.01E−01	1.70E−01	1.13E−01	2.57E−01	2.84E−01	2.76E−01	2.06E−01
	Z-score	3.41E−02	1.50E−02	3.23E−02	9.00E−03	−1.33E−02	−1.35E−02	−1.58E−02	−2.20E−02
Shortest path length-based	Average shortest path length	3.90E+00	4.01E+00	4.41E+00	4.06E+00	4.80E+00	4.79E+00	4.95E+00	5.04E+00
	Betweenness centrality	2.14E−03	1.00E−03	2.04E−03	0.00E+00	5.00E−04	0.00E+00	4.02E−04	0.00E+00
	Average closeness centrality	2.58E−01	2.50E−01	2.36E−01	2.46E−01	2.10E−01	2.09E−01	2.06E−01	1.99E−01
	Current flow betweenness	4.33E−03	3.00E−03	3.86E−03	2.00E−03	1.25E−03	1.00E−03	1.13E−03	1.00E−03
	Deviation	9.89E+03	1.07E+04	1.39E+04	1.11E+04	1.70E+04	1.69E+04	1.82E+04	1.89E+04
	Distance deviation	7.30E+03	6.47E+03	7.04E+03	6.61E+03	3.06E+03	3.89E+03	4.35E+03	4.16E+03
	Distance sum	3.11E+04	3.19E+04	3.51E+04	3.23E+04	3.82E+04	3.81E+04	3.94E+04	4.01E+04
	Eccentric	1.08E+00	1.34E+00	1.10E+00	1.34E+00	8.23E−01	6.60E−01	6.32E−01	6.60E−01
	Eccentricity	1.03E+01	1.00E+01	1.06E+01	1.00E+01	1.13E+01	1.20E+01	1.14E+01	1.10E+01
	Eccentricity dentrality	9.77E−02	1.00E−01	9.53E−02	1.00E−01	8.91E−02	8.30E−02	8.82E−02	9.10E−02
	Harmonic closeness centrality	2.21E+03	2.12E+03	2.00E+03	2.10E+03	1.76E+03	1.75E+03	1.72E+03	1.64E+03
	Load centrality	2.11E−03	1.00E−03	2.11E−03	0.00E+00	5.00E−04	0.00E+00	4.02E−04	0.00E+00
	Normalized betweenness	4.64E−03	2.00E−03	4.46E−03	1.00E−03	1.28E−03	1.00E−03	9.71E−04	0.00E+00
	Residual closeness centrality	6.77E+02	6.16E+02	5.49E+02	5.98E+02	3.78E+02	3.66E+02	3.58E+02	3.00E+02
	Radiality	8.18E−01	8.12E−01	7.87E−01	8.09E−01	7.63E−01	7.63E−01	7.53E−01	7.48E−01
	Stress	2.59E+06	9.00E+05	2.33E+06	4.81E+05	4.80E+05	3.25E+05	4.73E+05	2.08E+05
Biological system-based	Number of affiliated pathways	3.70E+00	3.00E+00	2.65E+00	3.00E+00	2.00E+00	2.00E+00	1.65E+00	2.00E+00
	Number of similarity proteins	1.35E+01	1.20E+01	9.55E+00	9.00E+00	2.33E+01	1.60E+01	1.05E+01	9.00E+00
	Number of target expression	1.48E−01	7.14E−04	2.79E−01	2.65E−01	4.23E−01	1.91E−01	2.81E−01	2.08E−01
	Number of tissue	3.69E+00	4.00E+00	3.06E+00	3.00E+00	3.78E+00	4.00E+00	2.63E+00	2.00E+00

Therefore, after a thorough investigation of 36 features, the 19 features were eventually merged into five features due to their innate interdependence. Considering the remaining 17 relatively independent features, a total of 22 features for each target were applied for further feature selection. The method of feature integration referred to previous research by our group [20], as well as the biological description and equation of those 36 properties in human PPI networks and biological system profiles, provided in Supplementary Table S1.

3.2. Revealing the essential properties of NTI drug targets in cancer by an artificial intelligence-based algorithm

The Boruta algorithm was built by an artificial intelligence method, which is particularly suitable for low-dimensional data sets compared to other available strategies because of its strong stability in variable selection [20,116]. Specifically, by setting the key parameters (described in detail in the Materials and Methods section), the R package Boruta was used to selecting the key difference features from 22 target profiles. The feature selection result is shown in Fig. 1, which means that 13 features were selected to collectively reflect the underlying mechanism of cancer NTI drugs, including 'interconnectivity', 'bridging coefficient', 'average shortest path length', 'average closeness centrality', 'radiality', 'topological coefficient', 'number of affiliated pathways', 'number of similarity proteins', 'stress', 'number of tissues', 'degree', 'neighborhood connectivity', and 'number of triangles'. The violin districts colored dark blue and light blue refer to the NTI drug targets in cancer and NNTI drug targets in all indications, respectively. Among these 13 selected features, some important features

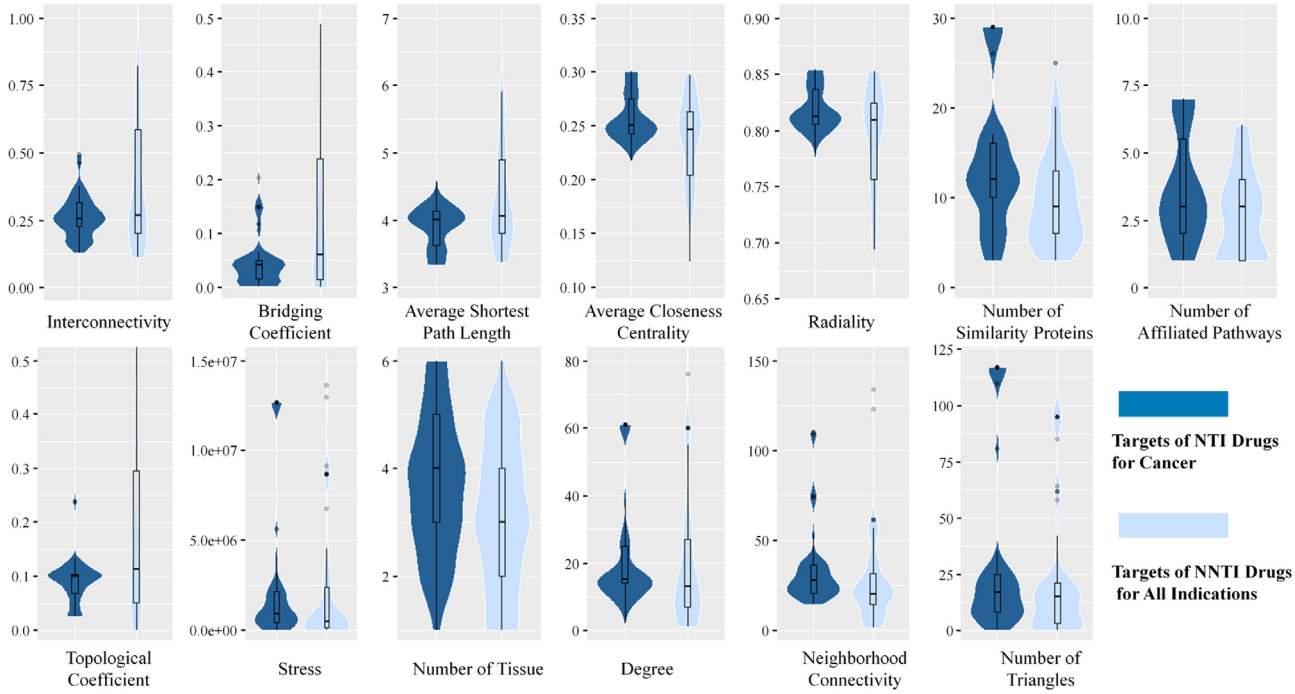

Fig. 1. Violin plot of the 13 features identified in cancer. For each feature, dark blue represents the targets of NTI drugs for cancer, and light blue represents the targets of NNTI drugs for all indications. (For interpretation of the references to colour in this figure legend, the reader is referred to the web version of this article.)

displayed an upward trend from NTI to NNTI drug targets (such as 'interconnectivity'), while others showed a downward trend (such as 'average closeness centrality'). In particular, the 'average closeness centrality' is defined as the reciprocal of the average shortest path length of the studied target. It measures how fast information spreads from a studied drug target to other reachable proteins in the PPI network [122], and the 'interconnectivity' is a connection metric that indicates the quality or status of the studied targets connected [123]. It was reported that a higher value of 'average closeness centrality' and a higher level (lower value) of 'interconnectivity' of the target demonstrated a greater lethality risk [20,124], which meant that a protein with tremendous centrality and connectivity carries a greater lethality risk. The results from our study proved that the capabilities of the applied Boruta algorithms in determining essential features of cancer NTI drug targets were due to the trends of the values of features in NTI and NNTI in Fig. 1, in agreement with these previous studies. Moreover, what we found also suggested that some features could be indirectly relevant to the drug risk-to-benefit ratio [124–125], and NTI drug targets of cancer in the biological network were not only inclined to be hub proteins [126] but also to have high centrality and connectivity.

3.3. Discovering the basic characteristics of NTI drug targets in cardiovascular disease by artificial intelligence-based algorithm

To identify the features of NTI drugs treating cardiovascular disease, the Boruta algorithm was adopted. The results are shown in Fig. 2. Eleven features were selected to collectively reflect the underlying mechanism of cardiovascular disease NTI drugs, including 'interconnectivity', 'bridging coefficient', 'average shortest path length', 'average closeness centrality', 'radiality', 'number of affiliated pathways', 'number of similarity proteins', 'topological coefficient', 'stress', 'number of tissues', and 'distance deviation'. In Fig. 2, the violin districts colored dark orange and light orange refers to the NTI drug targets in cardiovascular disease and NNTI drug targets in all indications, respectively. Similar to drug targets in cancer, some important features displayed an upward trend from NTI to NNTI drug targets (such as 'average shortest path length'). In contrast, some displayed a downward trend (such as 'radiality'). The 'average shortest path length' describes the average length of shortest paths between the studied drug target and all other proteins in the studied PPI network [127], and the 'radiality' is the reachability level of the studied nodes through diverse shortest paths throughout the network [128]. Moreover, the trend of these features in NTI and NNTI drug targets meant that NTI drug targets of cardiovascular disease were likely to have more links with other proteins. [129].

3.4. Exploring the shared/differential characteristics of NTI drug targets between cancers and cardiovascular diseases

The shared/differential features of NTI drug targets between cancers and cardiovascular diseases identified in the study are provided in Fig. 3. The boxes of pink background are the feature class of *Connectivity*, the boxes of light green background are the feature class of *Centrality*, and the box of yellow background provides the feature class of *Biological System Profile*. Besides, the dark blue bars indicated the characteristics of NTI drug targets for cancers, and the orange bars denoted the characteristics of NTI drug targets for cardiovascular diseases. Those 10 features in the first layer are shared by both cancers and cardiovascular diseases. Seven of these 10 features are the same as those identified by the previous report [20], which include 'average shortest path length', 'bridging coefficient', 'closeness centrality', 'interconnectivity', 'number of affiliated pathways', 'number of similarity proteins' and 'radiality'. These features indicated that the NTI drug targets of cancers and cardiovascular diseases were greatly connected and centralized in human PPI networks, and shared a biological system of the large number of similar proteins and target-affiliated pathways [20]. Moreover, these results validated the capability of *Boruta*

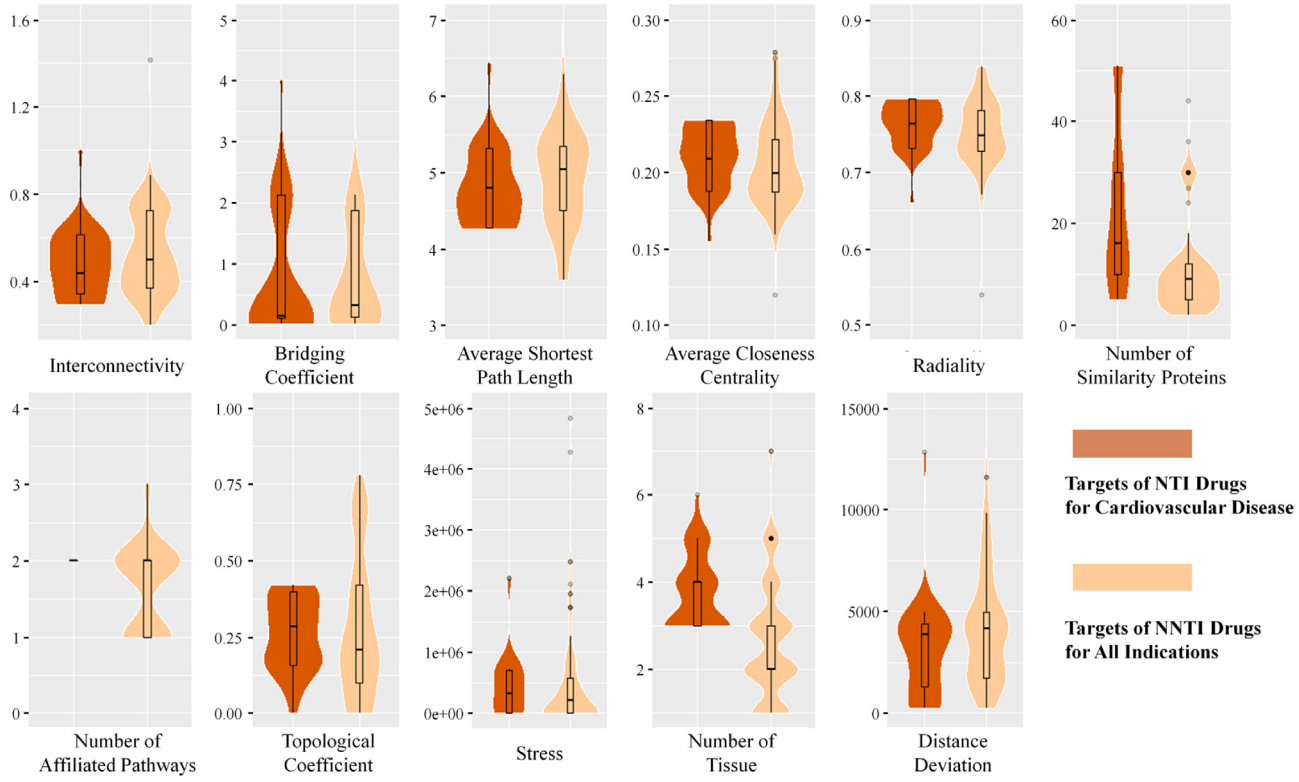

Fig. 2. Violin plot of the 11 features identified in cardiovascular disease. For each feature, dark orange represents the targets of NTI drugs for cardiovascular disease, and light orange represents the targets of NNTI drugs for all indications. (For interpretation of the references to colour in this figure legend, the reader is referred to the web version of this article.)

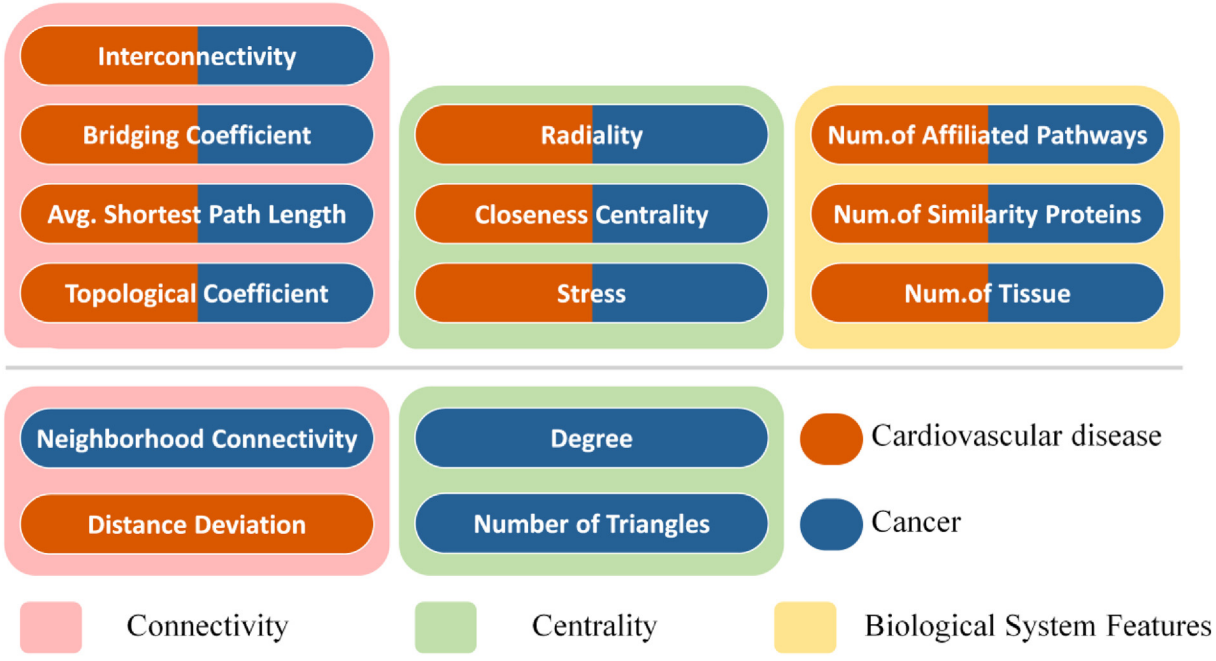

Fig. 3. Classification of the key features of cancer and cardiovascular disease determined in this study into three feature groups.

[114] in determining the features of NTI drug targets in different disease classes.

The second layer is unique characteristics identified for cancers (dark blue) and cardiovascular diseases (organge). For cancers, the identified features included 'neighborhood connectivity', 'degree', and 'number of triangles'. For cardiovascular diseases, the discovered feature was 'distance deviation'. As reported, drug targets tend to have a lower 'clustering coefficient' in cancer [15]. The 'clustering coefficient' denoted neighborhood connectivity [130], and the 'clustering coefficient' decreased with the increase in the

number of interacting proteins [131]. Therefore, a lower 'clustering coefficient' indicates higher 'neighborhood connectivity'. The 'degree' means the total number of edges connected to the studied node, and the 'number of triangles' that referred to the percentage of the triangle between a node and its neighbors. The higher the 'degree' and 'number of triangles', the higher the centrality of the drug target, and the more likely it is to lead to adverse drug reactions [132]. Thus, the computational discoveries of our result that cancer has a higher value of 'degree', 'number of triangles', and 'neighborhood connectivity' are consistent with literature reports. These phenomena indicate that the molecular mechanisms underlying of NTI drug targets in cancer require greater attention for the higher level of 'degree', 'number of triangles', and 'neighborhood connectivity'.

3.5. Clinical implication of the identified features underlying NTI drug targets

Based on the above analyses, a total of ten features from three feature groups were identified as common features for both disease classes (cancers & cardiovascular diseases) in distinguishing NTI from NNTI drug targets, and there were another 4 features from two feature groups that were singled out by one of those 2 disease classes. Those shared feature groups identified in this study were consistent with our previous publication [20], which reaffirmed the importance of these shared features in differentiating NTI drug targets from NNTI ones. Since the vast majority of all NTI drugs were from those two disease classes (cancers & cardiovascular diseases), it was not surprising to have such similarity in the shared feature groups. Such shared features could also provide a new direction for optimizing the drug efficacy-safety balance [20]. Particularly, the importance of these shared features in the prediction of drug-induced hepatotoxicity has already been reported by the previous publication [133].

More importantly, those features that were unique in different disease classes were concentrated in two feature classes of *Connectivity* and *Centrality*. Particularly, the features unique to cancer included 'degree', 'neighborhood connectivity', and 'number of triangles'. The 'degree' denoted the number of proteins in the human PPI network that interacted with the studied drug target [134]. The 'neighborhood connectivity' indicated the average number of interacting proteins of all the studied drug target's neighbors [135]. The 'number of triangles' showed the number of triangles that included the studied target as a vertex [136], and this triangular relationship includes the studied drug target and its interacting proteins, as well as the interactions among the interacting proteins. In fact, these three features could collectively represent whether the studied drug target acted as a hub in the human PPI network, the higher their values the stronger the core position of the studied targets [137]. These findings represent an emphasis by cancers in differentiating NTI drug targets with respect to the target's ability to be a hub in the PPI network. In other words, the narrow therapeutic index of an anticancer drug may originate from its interaction with hub protein [138–139]. To improve the situation of the narrow therapeutic index of anticancer drugs, it is necessary to impose more requirements on target selection. The hub proteins in the human PPI network should be avoided when designing anticancer drugs.

Different from cancers, the unique feature singled out in cardiovascular diseases is 'distance deviation', which belongs to the connectivity feature group. The 'distance deviation' indicated the absolute difference between the sum of all shortest paths starting from the studied target to all other proteins and the mean shortest path length of all the proteins in the human PPI network [135]. This implied an emphasis on the efficiency of inter-target signaling in NTI drug targets for cardiovascular diseases [135,140], which may indicate the needs for a more in-depth study of target signaling pathways when designing drugs for cardiovascular diseases. All in all, this study identified the key target features indicating the NTI drugs for cancers and cardiovascular diseases, which has great clinical implications in the drug designs for both disease classes.

4. Conclusion

This work is the first practice to reveal the underlying mechanism behind the complex definition and interpretation of NTI between different disease classes. Ten shared and four unique features were identified for both disease classes (cancers & cardiovascular diseases) to distinguish NTI drug targets from NNTI ones. This work suggested that in the clinical study of avoiding narrow therapeutic index in those diseases, the ability of target to be a hub and the efficiency of target signaling in the human PPI network should be especially considered.

Author contributions

Feng ZHU, Su ZENG conceived the idea and supervised the work. Jiayi YIN, Xiaoxu LI performed the research. Jiayi YIN, Xiaoxu LI and Fengcheng LI prepared and analyzed the data. Jiayi YIN, Xiaoxu LI, Yinjing LU, wrote the manuscript. All authors have read and approved this manuscript.

Funding

Funded by National Natural Science Foundation of China (81872798 & U1909208); Natural Science Foundation of Zhejiang Province (LR21H300001); National Key R&D Program of China (2018YFC0910500); Leading Talent of the 'Ten Thousand Plan' - National High-Level Talents Special Support Plan of China; Fundamental Research Fund for Central Universities (2018QNA7023); Key R&D Program of Zhejiang Province (2020C03010). This work was supported by Alibaba-Zhejiang University Joint Research Center of Future Digital Healthcare; Alibaba Cloud; Information Technology Center of Zhejiang University.

Declaration of Competing Interest

The authors declare that they have no known competing financial interests or personal relationships that could have appeared to influence the work reported in this paper.

Appendix A. Supplementary data

Supplementary data to this article can be found online at https://doi.org/10.1016/j.csbj.2021.04.035.

References

[1] Yu LX, Jiang W, Zhang X, Lionberger R, Makhlouf F, et al. Novel bioequivalence approach for narrow therapeutic index drugs. Clin Pharmacol Ther 2015;97(3):286–91.
[2] Muller PY, Milton MN. The determination and interpretation of the therapeutic index in drug development. Nat Rev Drug Discov 2012;11(10):751–61.
[3] Tamargo J, Le Heuzey JY, Mabo P. Narrow therapeutic index drugs: a clinical pharmacological consideration to flecainide. Eur J Clin Pharmacol 2015;71(5):549–67.
[4] Krens SD, Lassche G, Jansman FGA, Desar IME, et al. Dose recommendations for anticancer drugs in patients with renal or hepatic impairment. Lancet Oncol 2019;20(4):e200–7.
[5] Chen L, Chu C, Zhang Y-H, Zheng M, Zhu L, et al. Identification of drug-drug interactions using chemical interactions. Curr Bioinform 2017;12(6):526–34.
[6] Han H, Jain AD, Truica MI, Izquierdo-Ferrer J, Anker JF, et al. Small-molecule MYC inhibitors suppress tumor growth and enhance immunotherapy. Cancer Cell 2019;36(5):483–97.

[7] Sang SB, Guo X, Wang JZ, Li HM, Ma XY. Real-time and label-free detection of VKORC1 genes based on a magnetoelastic biosensor for warfarin therapy. J Mater Chem B 2020;8(29):6271–6.
[8] Subbiah V, Yang D, Velcheti V, Drilon A, Meric-Bernstam F. State-of-the-art strategies for targeting RET-dependent cancers. J Clin Oncol 2020;38(11):1209–21.
[9] Zaykov AN, Mayer JP, DiMarchi RD. Pursuit of a perfect insulin. Nat Rev Drug Discov 2016;15(6):425–39.
[10] Moreno L, Pearson ADJ, Paoletti X, Jimenez I, Geoerger B, et al. Early phase clinical trials of anticancer agents in children and adolescents - an ITCC perspective. Nat Rev Clin Oncol 2017;14(8):497–507.
[11] Dixit VA. A simple model to solve a drug toxicity problem. Toxicol Res 2019;8(2):157–71.
[12] Jakhar R, Dangi M, Khichi A, Chhillar AK. Relevance of molecular docking studies in drug designing. Curr Bioinform 2020;15(4):270–8.
[13] ten Freyhaus H, Dumitrescu D, Berghausen E, Vantler M, Caglayan E, et al. Imatinib mesylate for the treatment of pulmonary arterial hypertension. Expert Opin Investig Drugs 2012;21(1):119–34.
[14] Cai Y, Zhang X, Shen J, Jiang B, Hu D, et al. Heparin-binding protein: a novel biomarker linking four different cardiovascular diseases. Cardiol Res Pract 2020;2020:9575373.
[15] Sun J, Zhu K, Zheng W, Xu H. A comparative study of disease genes and drug targets in the human protein interactome. BMC Bioinf 2015;16(Suppl 5):S1.
[16] Hinrichs MJM, Ryan PM, Zheng B, Afif-Rider S, Yu XQ, et al. Fractionated dosing improves preclinical therapeutic index of pyrrolobenzodiazepine-containing antibody drug conjugates. Clin Cancer Res 2017;23(19):5858–68.
[17] Bottino DC, Patel M, Kadakia E, Zhou J, Patel C, et al. Dose pptimization for anticancer drug combinations: maximizing therapeutic index via clinical exposure-toxicity/preclinical exposure-efficacy modeling. Clin Cancer Res 2019;25(22):6633–43.
[18] Zhao X, Chen L, Guo Z-H, Liu T. Predicting drug side effects with compact integration of heterogeneous networks. Curr Bioinform 2019;14(8):709–20.
[19] Zhang L, Fang Y, Kopecek J, Yang J. A new construct of antibody-drug conjugates for treatment of B-cell non-Hodgkin's lymphomas. Eur J Pharm Sci 2017;103:36–46.
[20] Li XX, Yin J, Tang J, Li Y, Yang Q, et al. Determining the balance between drug efficacy and safety by the network and biological system profile of its therapeutic target. Front Pharmacol 2018;9:1245.
[21] Potega A, Zelaszczyk D, Mazerska Z. Electrochemical and in silico approaches for liver metabolic oxidation of antitumor-active triazoloacridinone C-1305. J Pharm Anal 2020;10(4):376–84.
[22] Drugs F. Pharmacometric approach to define narrow therapeutic index (NTI) drugs & evaluate bioequivalence (BE) criteria for NTI drugs. Drugs@FDA 2018;1(1):1–25.
[23] Bretagne M, Boudou-Rouquette P, Huillard O, Thomas-Schoemann A, Chahwakilian A, et al. Tyrosine kinase inhibiting the VEGF pathway and elderly people: Tolerance, pre-treatment assessment and side effects management. Bull Cancer 2016;103(3):259–72.
[24] Lin YS, Kerr SJ, Randolph T, Shireman LM, Senn T, et al. Prediction of intravenous busulfan clearance by endogenous plasma biomarkers using global pharmacometabolomics. Metabolomics 2016;12(10):161.
[25] Ciftci R, Tas F, Karabulut S, Ciftci S. Combination of capecitabine and phenytoin may cause phenytoin intoxication: a case report. Am J Ther 2015;22(1):e17–9.
[26] Rousseau A, Marquet P, Debord J, Sabot C, Lachatre G. Adaptive control methods for the dose individualisation of anticancer agents. Clin Pharmacokinet 2000;38(4):315–53.
[27] Onoda JM, Nelson KK, Taylor JD, Honn KV. Cisplatin and nifedipine: synergistic antitumor effects against an inherently cisplatin-resistant tumor. Cancer Lett 1988;40(1):39–47.
[28] Romano MJ, Dinh A. A 1000-fold overdose of clonidine caused by a compounding error in a 5-year-old child with attention-deficit/hyperactivity disorder. Pediatrics 2001;108(2):471–2.
[29] Ekhart C, Gebretensae A, Rosing H, Rodenhuis S, Beijnen JH, et al. Simultaneous quantification of cyclophosphamide and its active metabolite 4-hydroxycyclophosphamide in human plasma by high-performance liquid chromatography coupled with electrospray ionization tandem mass spectrometry. J Chromatogr B Analyt Technol Biomed Life Sci 2007;854(1–2):345–9.
[30] Gozalpour E, Greupink R, Bilos A, Verweij V, van den Heuvel JJ, et al. Convallatoxin: a new P-glycoprotein substrate. Eur J Pharmacol 2014;744:18–27.
[31] Henderson JD, Esham RH. Generic substitution: issues for problematic drugs. South Med J 2001;94(1):16–21.
[32] Valdes Jr R, Jortani SA, Gheorghiade M. Standards of laboratory practice: cardiac drug monitoring. National academy of clinical biochemistry. Clin Chem 1998;44(5):1096–109.
[33] Eckmann K, Michaud LB, Rivera E, Madden TL, Esparza-Guerra L, et al. Pilot study to assess toxicity and pharmacokinetics of docetaxel in patients with metastatic breast cancer and impaired liver function secondary to hepatic metastases. J Oncol Pharm Pract 2014;20(2):120–9.
[34] Han YL, Yu HL, Li D, Meng XL, Zhou ZY, et al. Inhibitory effects of limonin on six human cytochrome P450 enzymes and P-glycoprotein in vitro. Toxicol In Vitro 2011;25(8):1828–33.
[35] Simons FE. Epinephrine (adrenaline) in the first-aid, out-of-hospital treatment of anaphylaxis. Novartis Found Symp 2004;257:228–43.
[36] Cersosimo RJ, Hong WK. Epirubicin: a review of the pharmacology, clinical activity, and adverse effects of an adriamycin analogue. J Clin Oncol 1986;4(3):425–39.
[37] Najar IA, Johri RK. Pharmaceutical and pharmacological approaches for bioavailability enhancement of etoposide. J Biosci 2014;39(1):139–44.
[38] van Gelder T, Fischer L, Shihab F, Shipkova M. Optimizing everolimus exposure when combined with calcineurin inhibitors in solid organ transplantation. Transplant Rev 2017;31(3):151–7.
[39] Padhi D, Harris R. Clinical pharmacokinetic and pharmacodynamic profile of cinacalcet hydrochloride. Clin Pharmacokinet 2009;48(5):303–11.
[40] Saif MW, Diasio RB. Benefit of uridine triacetate (vistogard) in rescuing severe 5-fluorouracil toxicity in patients with dihydropyrimidine dehydrogenase (DPYD) deficiency. Cancer Chemother Pharmacol 2016;78(1):151–6.
[41] Fareed J, Hoppensteadt DA, Bick RL. Management of thrombotic and cardiovascular disorders in the new millenium. Clin Appl Thromb Hemost 2003;9(2):101–8.
[42] Thirukkumaran C, Morris DG. Oncolytic viral therapy using reovirus. Methods Mol Biol 2015;1317:187–223.
[43] Mercier C, Raynal C, Dahan L, Ortiz A, Evrard A, et al. Toxic death case in a patient undergoing gemcitabine-based chemotherapy in relation with cytidine deaminase downregulation. Pharmacogenet Genomics 2007;17(10):841–4.
[44] Pogue SL, Taura T, Bi M, Yun Y, Sho A, et al. Targeting attenuated interferon-alpha to myeloma cells with a CD38 antibody induces potent tumor regression with reduced off-target activity. PLoS ONE 2016;11(9):e0162472.
[45] Parker BM, Cusack BJ, Vestal RE. Pharmacokinetic optimisation of drug therapy in elderly patients. Drugs Aging 1995;7(1):10–8.
[46] Sahasranaman S, Howard D, Roy S. Clinical pharmacology and pharmacogenetics of thiopurines. Eur J Clin Pharmacol 2008;64(8):753–67.
[47] Shah IA, Lindup WE, McCulloch PG. Variability of mitomycin C adsorption by activated charcoal. J Pharm Pharmacol 1998;50(3):251–6.
[48] Theile D, Haefeli WE, Weiss J. Effects of adrenolytic mitotane on drug elimination pathways assessed in vitro. Endocrine 2015;49(3):842–53.
[49] Hwang SJ, Park JW, Lee SD, Kim GJ, Sin CH, et al. Capecitabine and oxaliplatin (XELOX) for the treatment of patients with metastatic gastric cancer and severe liver dysfunction. Korean J Intern Med 2006;21(4):252–5.
[50] Minhas S, Setia N, Pandita S, Saxena R, Verma IC, et al. Prevalence of CYP2C8 polymorphisms in a North Indian population. Genet Mol Res 2013;12(3):2260–6.
[51] Posada MM, Bacon JA, Schneck KB, Tirona RG, Kim RB, et al. Prediction of renal transporter mediated drug-drug interactions for pemetrexed using physiologically based pharmacokinetic modeling. Drug Metab Dispos 2015;43(3):325–34.
[52] Umer Usman MH, Raza S, Raza S, Ezekowitz M. Advancement in antithrombotics for stroke prevention in atrial fibrillation. J Interv Card Electrophysiol 2008;22(2):129–37.
[53] Kuhn MA. Herbal remedies: drug-herb interactions. Crit Care Nurse 2002;22(2):22–8.
[54] Said R, Tsimberidou AM. Pharmacokinetic evaluation of vincristine for the treatment of lymphoid malignancies. Expert Opin Drug Metab Toxicol 2014;10(3):483–94.
[55] Ibrahim NK, Valero V, Rahman Z, Theriault RL, Walters RS, et al. Phase I-II vinorelbine (navelbine) by continuous infusion in patients with metastatic breast cancer: cumulative toxicities limit dose escalation. Cancer Invest 2001;19(5):459–66.
[56] Mullard A. 2012 FDA drug approvals. Nat Rev Drug Discov 2013;12(2):87–90.
[57] Carstairs SD, Williams SR. Overdose of aripiprazole, a new type of antipsychotic. J Emerg Med 2005;28(3):311–3.
[58] Spencer T, Biederman J, Wilens T. Nonstimulant treatment of adult attention-deficit/hyperactivity disorder. Psychiatr Clin North Am 2004;27(2):373–83.
[59] Mullard A. 2011 FDA drug approvals. Nat Rev Drug Discov 2012;11(2):91–4.
[60] Verbeeck RK, Kanfer I, Lobenberg R, Abrahamsson B, Cristofoletti R, et al. Biowaiver monographs for immediate-release solid oral dosage forms: enalapril. J Pharm Sci 2017;106(8):1933–43.
[61] Walia KS, Khan EA, Ko DH, Raza SS, Khan YN. Side effects of antiepileptics–a review. Pain Pract 2004;4(3):194–203.
[62] Hughes B. 2008 FDA drug approvals. Nat Rev Drug Discov 2009;8(2):93–6.
[63] Strauch S, Jantratid E, Dressman JB, Junginger HE, Kopp S, et al. Biowaiver monographs for immediate release solid oral dosage forms: lamivudine. J Pharm Sci 2011;100(6):2054–63.
[64] Graefe-Mody U, Retlich S, Friedrich C. Clinical pharmacokinetics and pharmacodynamics of linagliptin. Clin Pharmacokinet 2012;51(7):411–27.
[65] Eklund JW, Trifilio S, Mulcahy MF. Chemotherapy dosing in the setting of liver dysfunction. Oncology (Williston Park) 2005;19(8):1057–63.
[66] Saletan S. Mitoxantrone: an active, new antitumor agent with an improved therapeutic index. Cancer Treat Rev 1987;14(3–4):297–303.
[67] Knorr B, Franchi LM, Bisgaard H, Vermeulen JH, LeSouef P, et al. Montelukast, a leukotriene receptor antagonist, for the treatment of persistent asthma in children aged 2 to 5 years. Pediatrics 2001;108(3):E48.
[68] Eichenfield LF, Beck L. Elidel (pimecrolimus) cream 1%: a nonsteroidal topical agent for the treatment of atopic dermatitis. J Allergy Clin Immunol 2003;111(5):1153–68.
[69] Hot drugs 2004. Nat Rev Drug Discov. 2004;Suppl:S3-40.
[70] Wang X, Zhang ZY, Arora S, Hughes L, Wang J, et al. Effects of rolapitant administered intravenously or orally on the pharmacokinetics of digoxin (P-

glycoprotein substrate) and sulfasalazine (breast cancer resistance protein substrate) in healthy volunteers. J Clin Pharmacol 2018;58(2):202–11.
[71] Hughes B. 2009 FDA drug approvals. Nat Rev Drug Discov 2010;9(2):89–92.
[72] Schwartz LM, Woloshin S, Zheng E, Tse T, Zarin DA. ClinicalTrials.gov and Drugs@FDA: a comparison of results reporting for new drug approval trials. Ann Intern Med 2016;165(6):421–30.
[73] The L. ICD-11. Lancet 2019;393(10188):2275.
[74] Wang Y, Zhang S, Li F, Zhou Y, Zhang Y, et al. Therapeutic target database 2020: enriched resource for facilitating research and early development of targeted therapeutics. Nucleic Acids Res 2020;48(D1):D1031–41.
[75] Szklarczyk D, Gable AL, Lyon D, Junge A, Wyder S, et al. STRING v11: protein-protein association networks with increased coverage, supporting functional discovery in genome-wide experimental datasets. Nucleic Acids Res 2019;47(D1):D607–13.
[76] Ghosh S, Kumar GV, Basu A, Banerjee A. Graph theoretic network analysis reveals protein pathways underlying cell death following neurotropic viral infection. Sci Rep 2015;5:14438.
[77] Liu K, Wang ZQ, Wang SJ, Liu P, Qin YH, et al. Hyaluronic acid-tagged silica nanoparticles in colon cancer therapy: therapeutic efficacy evaluation. Int J Nanomedicine 2015;10:6445–54.
[78] Zhang P, Tao L, Zeng X, Qin C, Chen S, et al. A protein network descriptor server and its use in studying protein, disease, metabolic and drug targeted networks. Brief Bioinform 2017;18(6):1057–70.
[79] Shannon P, Markiel A, Ozier O, Baliga NS, Wang JT, et al. Cytoscape: a software environment for integrated models of biomolecular interaction networks. Genome Res 2003;13(11):2498–504.
[80] Thomas S, Bonchev D. A survey of current software for network analysis in molecular biology. Hum Genomics 2010;4(5):353–60.
[81] Kanehisa M, Furumichi M, Sato Y, Ishiguro-Watanabe M, Tanabe M. KEGG: integrating viruses and cellular organisms. Nucleic Acids Res 2021;49(D1):D545–51.
[82] Kogenaru S, del Val C, Hotz-Wagenblatt A, Glatting KH. TissueDistributionDBs: a repository of organism-specific tissue-distribution profiles. Theor Chem Acc 2010;125(3–6):651–8.
[83] UniProt C. UniProt: a worldwide hub of protein knowledge. Nucleic Acids Res 2019;47(D1):D506–15.
[84] Zheng CJ, Han LY, Yap CW, Ji ZL, Cao ZW, et al. Therapeutic targets: progress of their exploration and investigation of their characteristics. Pharmacol Rev 2006;58(2):259–79.
[85] Zhu F, Han L, Zheng C, Xie B, Tammi MT, et al. What are next generation innovative therapeutic targets? Clues from genetic, structural, physicochemical, and systems profiles of successful targets. J Pharmacol Exp Ther 2009;330(1):304–15.
[86] Song L, Xu W, Li C, Li H, Wu L, et al. Development of expressed sequence tags from the bay scallop. Argopecten irradians irradians Mar Biotechnol (NY) 2006;8(2):161–9.
[87] Singh S, Malik BK, Sharma DK. Choke point analysis of metabolic pathways in E.histolytica: a computational approach for drug target identification. Bioinformation 2007;2(2):68–72.
[88] Yin J, Sun W, Li F, Hong J, Li X, et al. VARIDT 1.0: variability of drug transporter database. Nucleic Acids Res 2020;48(D1):D1042–50.
[89] Yin J, Li F, Zhou Y, Mou M, Lu Y, et al. INTEDE: interactome of drug-metabolizing enzymes. Nucleic Acids Res 2021;49(D1):D1233–43.
[90] Li YH, Yu CY, Li XX, Zhang P, Tang J, et al. Therapeutic target database update 2018: enriched resource for facilitating bench-to-clinic research of targeted therapeutics. Nucleic Acids Res 2018;46(D1):D1121–7.
[91] Barrett T, Wilhite SE, Ledoux P, Evangelista C, Kim IF, et al. NCBI GEO: archive for functional genomics data sets–update. Nucleic Acids Res 2013;41(D1):D991–5.
[92] Higueruelo AP, Jubb H, Blundell TL. Protein-protein interactions as druggable targets: recent technological advances. Curr Opin Pharmacol 2013;13(5):791–6.
[93] Rao HB, Zhu F, Yang GB, Li ZR, Chen YZ. Update of PROFEAT: a web server for computing structural and physicochemical features of proteins and peptides from amino acid sequence. Nucleic Acids Res. 2011;39(Web Server issue):W385-90.
[94] Xu J, Wang P, Yang H, Zhou J, Li Y, et al. Comparison of FDA approved kinase targets to clinical trial ones: insights from their system profiles and drug-target interaction networks. Biomed Res Int 2016;2016:2509385.
[95] Li YH, Li XX, Hong JJ, Wang YX, Fu JB, et al. Clinical trials, progression-speed differentiating features and swiftness rule of the innovative targets of first-in-class drugs. Brief Bioinform 2020;21(2):649–62.
[96] Huang LH, He QS, Liu K, Cheng J, Zhong MD, et al. ADReCS-Target: target profiles for aiding drug safety research and application. Nucleic Acids Res 2018;46(D1):D911–7.
[97] Issa NT, Stathias V, Schurer S, Dakshanamurthy S. Machine and deep learning approaches for cancer drug repurposing. Semin Cancer Biol 2021;68:132–42.
[98] Liu J, Lian X, Liu F, Yan X, Cheng C, et al. Identification of novel key targets and candidate drugs in oral squamous cell carcinoma. Curr Bioinform 2020;15(4):328–37.
[99] Yang Q, Li B, Tang J, Cui X, Wang Y, et al. Consistent gene signature of schizophrenia identified by a novel feature selection strategy from comprehensive sets of transcriptomic data. Brief Bioinform 2020;21(3):1058–68.
[100] Tang J, Fu J, Wang Y, Li B, Li Y, et al. ANPELA: analysis and performance assessment of the label-free quantification workflow for metaproteomic studies. Brief Bioinform 2020;21(2):621–36.
[101] Yang Q, Wang Y, Zhang Y, Li F, Xia W, et al. NOREVA: enhanced normalization and evaluation of time-course and multi-class metabolomic data. Nucleic Acids Res 2020;48(W1):W436–48.
[102] Romm EL, Tsigelny IF. Artificial intelligence in drug treatment. Annu Rev Pharmacol Toxicol 2020;60:353–69.
[103] Tang J, Mou M, Wang Y, Luo Y, Zhu F. MetaFS: Performance assessment of biomarker discovery in metaproteomics. Brief Bioinform 2020. https://doi.org/10.1093/bib/bbaa105.
[104] Marya NB, Powers PD, Fujii-Lau L, Abu Dayyeh BK, Gleeson FC, et al. Application of artificial intelligence using a novel EUS-based convolutional neural network model to identify and distinguish benign and malignant hepatic masses. Gastrointest Endosc 2020. https://doi.org/10.1016/j.gie.2020.08.024.
[105] Li Z, Wang Y, Tai S, Wang J, Huang Y, et al. APP medical diagnostic check-up consultation system based on speech recognition. Curr Bioinform 2020;15(5):408–14.
[106] Tang J, Fu J, Wang Y, Luo Y, Yang Q, et al. Simultaneous improvement in the precision, accuracy, and robustness of label-free proteome quantification by optimizing data manipulation chains. Mol Cell Proteomics 2019;18(8):1683–99.
[107] Kwon E, Cho M, Kim H, Son HS. A study on host tropism determinants of influenza virus using machine learning. Curr Bioinform 2020;15(2):121–34.
[108] Xue W, Yang F, Wang P, Zheng G, Chen Y, et al. What contributes to serotonin-norepinephrine reuptake inhibitors' dual-targeting mechanism? The key role of transmembrane domain 6 in human serotonin and norepinephrine transporters revealed by molecular dynamics simulation. ACS Chem Neurosci 2018;9(5):1128–40.
[109] Li F, Zhou Y, Zhang X, Tang J, Yang Q, et al. SSizer: determining the sample sufficiency for comparative biological study. J Mol Biol 2020;432(11):3411–21.
[110] van der Burgh HK, Schmidt R, Westeneng HJ, de Reus MA, van den Berg LH, et al. Deep learning predictions of survival based on MRI in amyotrophic lateral sclerosis. Neuroimage Clin 2017;13:361–9.
[111] Seo S, Oh M, Park Y, Kim S. DeepFam: deep learning based alignment-free method for protein family modeling and prediction. Bioinformatics 2018;34(13):i254–62.
[112] Wang J, Wang H, Wang X, Chang H. Predicting drug-target interactions via FM-DNN learning. Curr Bioinform 2020;15(1):68–76.
[113] Krittanawong C, Zhang H, Wang Z, Aydar M, Kitai T. Artificial intelligence in precision cardiovascular medicine. J Am Coll Cardiol 2017;69(21):2657–64.
[114] Kursa MB. Robustness of random forest-based gene selection methods. BMC Bioinf 2014;15:8.
[115] Pan Y, Wang Z, Zhan W, Deng L. Computational identification of binding energy hot spots in protein-RNA complexes using an ensemble approach. Bioinformatics 2018;34(9):1473–80.
[116] Degenhardt F, Seifert S, Szymczak S. Evaluation of variable selection methods for random forests and omics data sets. Brief Bioinform 2019;20(2):492–503.
[117] Tang J, Wang Y, Luo Y, Fu J, Zhang Y, et al. Computational advances of tumor marker selection and sample classification in cancer proteomics. Comput Struct Biotechnol J 2020;18:2012–25.
[118] Shang L, Liu C, Tomiura Y, Hayashi K. Machine-learning-based olfactometer: prediction of odor perception from physicochemical features of odorant molecules. Anal Chem 2017;89(22):11999–2005.
[119] Ragusa M, Avola G, Angelica R, Barbagallo D, Guglielmino MR, et al. Expression profile and specific network features of the apoptotic machinery explain relapse of acute myeloid leukemia after chemotherapy. BMC Cancer 2010;10:377.
[120] Guo R, Zhang X, Su J, Xu H, Zhang Y, et al. Identifying potential quality markers of Xin-Su-Ning capsules acting on arrhythmia by integrating UHPLC-LTQ-orbitrap, ADME prediction and network target analysis. Phytomedicine 2018;44:117–28.
[121] Fathima AJ, Murugaboopathi G, Selvam P. Pharmacophore mapping of ligand based virtual screening, molecular docking and molecular dynamic simulation studies for finding potent NS2B/NS3 protease inhibitors as potential anti-dengue drug compounds. Curr Bioinform 2018;13(6):606–16.
[122] Ma B, Wang HZ, Dsouza M, Lou J, He Y, et al. Geographic patterns of co-occurrence network topological features for soil microbiota at continental scale in eastern China. Isme J 2016;10(8):1891–901.
[123] Emig D, Ivliev A, Pustovalova O, Lancashire L, Bureeva S, et al. Drug target prediction and repositioning using an integrated network-based approach. PLoS ONE 2013;8(4):e60618.
[124] Chen L, Wang Q, Zhang L, Tai J, Wang H, et al. A novel paradigm for potential drug-targets discovery: quantifying relationships of enzymes and cascade interactions of neighboring biological processes to identify drug-targets. Mol Biosyst 2011;7(4):1033–41.
[125] Muhammad J, Khan A, Ali A, Fang L, Yanjing W, et al. Network pharmacology: exploring the resources and methodologies. Curr Top Med Chem 2018;18(12):949–64.
[126] Wu CC, Kannan K, Lin S, Yen LS, Milosavljevic A. Identification of cancer fusion drivers using network fusion centrality. Bioinformatics 2013;29(9):1174–81.

[127] Wang C, Gong BS, Bushel PR, Thierry-Mieg J, Thierry-Mieg D, et al. The concordance between RNA-seq and microarray data depends on chemical treatment and transcript abundance. Nat Biotechnol 2014;32(9):926–32.
[128] Scardoni G, Petterlini M, Laudanna C. Analyzing biological network parameters with CentiScaPe. Bioinformatics 2009;25(21):2857–9.
[129] Zhang LC, Li X, Tai JX, Li W, Chen LN. Predicting candidate genes based on combined network topological features: a case study in coronary artery disease. PLoS ONE 2012;7(6):e39542.
[130] Modos D, Bulusu KC, Fazekas D, Kubisch J, Brooks J, et al. Neighbours of cancer-related proteins have key influence on pathogenesis and could increase the drug target space for anticancer therapies. NPJ Syst Biol Appl 2017;3:2.
[131] Kar G, Gursoy A, Keskin O. Human cancer protein-protein interaction network: a structural perspective. PLoS Comput Biol 2009;5(12):e1000601.
[132] Ma XJ, Ma YH. The local triangle structure centrality method to rank nodes in networks. Complex 2019;9057194.
[133] Xu L, Liang G, Liao C, Chen GD, Chang CC. k-Skip-n-Gram-RF: a random forest based method for alzheimer's disease protein identification. Front Genet 2019;10:33.
[134] Lawyer G. Understanding the influence of all nodes in a network. Sci Rep 2015;5:8665.
[135] Zhang P, Tao L, Zeng X, Qin C, Chen SY, et al. PROFEAT update: a protein features web server with added facility to compute network descriptors for studying omics-derived networks. J Mol Biol 2017;429(3):416–25.
[136] Rubinov M, Sporns O. Complex network measures of brain connectivity: uses and interpretations. Neuroimage 2010;52(3):1059–69.
[137] Wheeler H, Woods RL, Page J, Levi J. A phase II study of mitoxantrone in advanced squamous cell cancer of the head and neck. Invest New Drugs 1990;8(1):109–11.
[138] Jeong H, Mason SP, Barabasi AL, Oltvai ZN. Lethality and centrality in protein networks. Nature 2001;411(6833):41–2.
[139] Barabasi AL, Oltvai ZN. Network biology: understanding the cell's functional organization. Nat Rev Genet 2004;5(2):101–13.
[140] Embar V, Handen A, Ganapathiraju MK. Is the average shortest path length of gene set a reflection of their biological relatedness?. J Bioinform Comput Biol 2016;14(6):1660002.